View Article Online / Journal Homepage / Table of Contents for this issue

Photochemically induced increase in endothelial permeablity regulated by RhoA activation

Hiroki Ota, Mimiko Matsumura, Norihisa Miki and Haruyuki Minamitami

Received 26th March 2009, Accepted 10th July 2009
First published as an Advance Article on the web 29th July 2009
DOI: 10.1039/b906028f

Published on 29 July 2009. Downloaded by University of California - Berkeley on 12/01/2015 00:05:04.

Photochemical reactions used in photodynamic therapy are reported to damage normal cells and tissues in ways that increase endothelial permeability and thereby cause excessive neointimal formation and subsequent restenosis. To investigate the mechanisms of this permeability increase *in vitro*, human umbilical vein endothelial cells were incubated with the porphyrin precursor δ-aminolevulinic acid and then irradiated with a 646 nm light-emitting diode (LED). Results using Transwells® supports showed that the photochemical reaction increased endothelial permeability by 200%, and fluorescence microscopy revealed that destruction of the capillary-like structures due to cell shrinkage was accompanied by VE-cadherin mislocalization and stress fiber formation. The generated gaps between cells were observed using dyed β1-integrin and total internal reflection fluorescence microscopy. Western blotting indicated that the photochemical reaction phosphorylated GDP-RhoA to GTP-RhoA, a protein that promotes stress fiber formation and inhibits VE-cadherin production. When forskolin/rolipram or 8CPT-2′O-Me-cAMP, both of which inhibit further reaction of phosphorylated RhoA, were added, no formation of stress fibers or mislocalization of VE-cadherin was observed, thus preventing an increase in endothelial permeability. Taken together, photochemically induced RhoA activation appears to play a key role in increasing endothelial permeability during changes in morphology of endothelial cells.

Introduction

Photosensitizer-based photochemical reactions have been used in photodynamic therapy (PDT) for decades, and photosensitizer-based PDT has been making significant progress since Lipton developed an oncotropic photosensitizer in 1961.[1] PDT is an approved treatment for a number of diseases—including malignant glioma, atheroselerosis, and melanoma—and is expected to be used in the diagnosis and treatments of choroidal neovascularization and other cancers.

PDT is based on the light-induced activation of a photosensitizer, generating highly reactive oxygen species (ROS), in particular singlet oxygen. The photosensitizer is excited from the singlet ground state ^{1}S to the triplet excited state ^{3}T* by light irradiation, and the decay of that state to the ^{1}S state activates surrounding oxygen by exciting it from the triplet ground state to the singlet excited state.

δ-Aminolevulinic acid (ALA) is ofen used in PDT as a precursor of the photosensitizer protoporphyrin IX (PpIX). ALA-based PDT was reported first by Malik and Lugaci in 1987[2] followed by a clinical trial in 1990.[3] ALA itself is not harmful and is produced naturally in the course of heme production, in which the last step involves incorportion of iron to PpIX *via* ferrochelatase. Supplementation of exogenous ALA in the cells over-produces PpIX that exceeds the capacity of ferrochelatase, leading to its accumulation at high levels. Because ALA is attracted to neoplasmic rather than normal tissue, such excess PpIX preferentially accumulates in neoplasmic tissue.

Graduate School of Science and Technology, KEIO University, Japan

ROS produced by photochemical reactions in mitochondria or organelles directly cause cellular necrosis and apoptosis by disrupting enzymatic systems and signaling networks,[4] and also cause a vascular shutdown that results in lack of nutrition and tumor death.[5] Vascular shutdown is reported to be effective therapy for age-related macular degeneration.[6] However, *in vivo* evidence suggests that an increase in endothelial permeability, which was thought to originate from endothelial barrier breakdown caused by photochemical reactions, culminated in the deposition of the extracellular matrix in the neointima and/or in the proliferation of smooth muscle cells, resulting in luminal narrowing as a side effect of PDT.[7,8]

This study investigated ALA in human umbilical vein endothelial cells (HUVEC) *in vitro* to elucidate the mechanisms behind the increase in endothelial permeability and to identify the proteins associated with this process. This study may help in the design of a more effective PDT with less side effects.

Materials and methods

HUVEC and EGM-2 culture media were purchased from Cambrex. ALA was purchased from Funakoshi Co.. Hydrochloric acid, FITC-dextran, methanol, Triton X-100, MCDB-131, and paraformaldehyde were purchased from Sigma. PpIX was purchased from Alexis. Thiazolyl blue tetrazolium bromide (MTT) and calcein-AM were purchased from Dojindo Laboratories. Dulbecco's phosphate buffered saline was purchased from Gibco. Dimethyl sulfoxide (DMSO), sodium hydroxide, sodium bicarbonate, and HEPES were purchased from Wako. Cellmatrix Type I-A was purchased from Nitta Gelatin. Alexa Fluor®

View Article Online

Published on 29 July 2009. Downloaded by University of California - Berkeley on 12/01/2015 00:05:04.

568 phalloidin, DNaseI, and Alexa Fluor® 488 conjugate were purchased from Molecular Probe. Phenylmethylsulfonyl fluoride, sodium n-dodecyl sulfate (SDS), and Tween 20 were purchased from Kanto Chemical Co. Protein assay dye reagent was perchased from Bio-Rad. Anti-mouse IgG, HRP-linked whole antibody was purchased from Amersham. Western lightning chemiluminescence reagent was purchased from PerkinElmer Life Science. RhoA activation assay Biochem Kit™ was purchased from Cytoskeleton, Inc.

Measurement of cellular PpIX content

PpIX was extracted and measured as previously reported.[9] HUVEC were incubated in EGM-2 supplemented with 0–3 mM ALA in a 24-well plate for 4 h, rinsed with PBS, and then scraped off with a rubber policeman. These cells were mixed with 1 M HCl–CH_3OH and centrifuged at 4 °C. The supernatant was collected and inspected with a spectrofluorometer (ex. 405 nm, em. 620 nm) (RF 1500, Shimadzu).

Intracellular PpIX was detected by a confocal laser microscopy (LSM410, Carl Zeiss) with a 450–490 nm excitation filter and an emission filter passing wavelengths longer than 630 nm. Fluorescence images were acquired with a CCD camera (ORCA-ER, Hamamatsu Photonics).

ALA photochemical reaction treatment

After HUVEC were incubated in EGM-2 supplemented with 1 mM ALA in 24-well plates for 4 h, they were irradiated with a 646 nm light for 10 min using 280 arrays of red LEDs (Agilent Technologies) as a light source (Fig. 1). The output power of the light was adjusted to 10 mW cm^{-2} as measured with an optical power multimeter (Advantest).

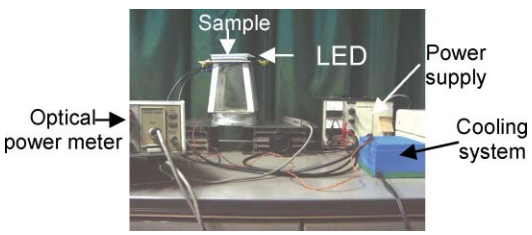

Fig. 1 LED light irradiation.

MTT viability assay

Phototoxicity was evaluated using MTT. Approximately 2×10^5 cells in fresh medium were seeded onto a 24-well plate and 24 h later exposed to the photoreaction irradiation. MTT was added to each well 24 h after the photoreaction and the samples were incubated at 37 °C for 4 h. After washing and dissolving of formazan with DMSO (200 µl per well), 100 µl samples were transferred to a 96-well plate and the optical density was measured using a microplate reader (MPR-A4i, Tosoh).

Permeability assay

The permeability of endothelial cell monolayers was measured using Corning Costar Transwell® supports with 3 µm pores. Approximately 2×10^5 cells in fresh medium were seeded onto the support in the 24-well plate and cultured until they formed a complete monolayer. FITC-dextran (1 mg mL^{-1}, average molecular weight = 40 000) was added to the upper chamber with the cells that had been treated without (control) or with the photoreaction irradiation. Each 25 µl sample was taken from the lower compartment and the fluorescence was measured with a spectrofluorometer (ex. 492 nm, em. 515 nm).

Formation of capillary-like structures of HUVEC

Capillary-like structures of HUVEC were formed by culturing the cells three-dimensionally in a collagen gel matrix. In each dish, 1.5×10^5 cells per ml were seeded onto collagen gels and incubated for 4 h to allow for adherence to the gels. The medium was removed and then the three layers of collagen gels were assembled. The cells were incubated for 30 min before fresh medium was added to the dishes.

Morphological analysis of subendothelial area

The cytoplasm of HUVEC was stained with calcein-AM to observe cell morphology. The cells were incubated with 10 µM calcein-AM and observed using fluorescence microscopy (Eclipse TE2000, Nikon). RGB images acquired by a CCD camera (DC120 Zoom, Kodak) were converted to gray-scale images using Image-Pro software (Roper Industries). Binary images were produced by thresholding the gray-scale images, and the subendothelial area that was displayed in black was measured using Image Pro.

F-actin, VE-cadherin and β1-integrin imaging

Cullere *et al.* verified the relationship between VE-cadherin mislocalization and endothelial permeability by immunofluorometry.[10] Cells were fixed for 1 h in 4% paraformaldehyde at 4 °C. The cells were first washed twice in PBS, then permeabilized in 0.1% Triton X-100 for 5 min, and again rinsed twice in PBS. For visualization of F-actin, the cells were stained for 20 min at room temperature with an 8 U ml^{-1} solution of Alexa Fluor® 568 phalloidin. For visualization of VE-cadherin and β1-integrin, cells were labeled for 60 min with the primary antibodies dissolved in PBS, washed twice with PBS, and then labeled for 45 min with fluorescein-conjugated affinity-purified donkey anti-mouse IgG absorbed for dual labeling secondary antibody. Fluorescence images of F-actin and VE-cadherin were acquired by confocal laser microscopy with a CSU21 (Yokogawa). As basal cells can be observed by total-internal-reflection fluorescence (TIRF) microscopy at high magnification with much less background noise than by conventional fluorescence microscopy, fluorescence images of β1-integrin were acquired by TIRF microscopy (TE200-U, Nikon). All the images were recorded with a CCD camera (ORCA-ER, Hamamatsu Photonics).

Western blotting

Western blotting was used for total RhoA analysis. Cells were washed with HBSS and immediately scraped in HBSS with a rubber policeman. Protein concentrations in the whole cell lysates were determined by the BCA protein assay. 100 µl of samples were lysed in a SDS sample buffer and an ice-cold lysis buffer and then resolved by SDS-PAGE and transferred to Hybond-P.

 This journal is © The Royal Society of Chemistry and Owner Societies 2009

View Article Online

Published on 29 July 2009. Downloaded by University of California - Berkeley on 12/01/2015 00:05:04.

The transferred samples were incubated with a RhoA antibody, followed by anti-mouse IgG HRP-linked whole antibody as the second antibody. The immunoblotted proteins were visualized with enhanced chemiluminescence reagents.

Measurement of RhoA activation

Active GTP-RhoA binds specifically to rhotekin-Rho-binding domain protein agarose beads that can be collected from endogenous lysates by centrifugation. The amount of phosphorylated RhoA was measured by western blotting. Photosensitized cells and untreated control cells were lysed in a buffer containing protease inhibitors. A small amount of each cell lysate was kept for total RhoA analysis, and the remaining lysate was incubated with rhotekin binding domain agarose for 1 h at 4 °C before centrifugation to pull down the GTP-RhoA beads. After the collected beads were washed in an assay buffer and resuspended in a sample buffer in the kit, the eluted protein was analyzed by western blotting using a RhoA antibody.

Statistical analysis

Data were expressed as means ± SD. The significant difference was assessed by the Student's *t*-test. Values of $P < 0.05$ were considered significant.

Results

Cellular PpIX content and phototoxicity

Porphyrin synthesis in HUVEC as measured by fluorescence intensity of PpIX was evaluated with respect to the amount of ALA added to the cells (Fig. 2a). Synthesis was dose-dependent with a peak at 1 mM ALA. Optical and fluorescence images of HUVEC before and after treatment with 1 mM ALA (Fig. 2b–e) showed PpIX accumulation in the cytoplasm.

The cytotoxicity of the photochemical reaction was assessed using MTT on cells 24 h after irradiation at 10 mW cm^{-2}. Cell viability of HUVEC did not decrease significantly with ALA concentrations of up to 5 mM (Fig. 3).

As PpIX accumulation was increased until the amount of ALA reached 1 mM and then plateaued, and as cell injury was minimal, the following experiments were preformed using 1 mM ALA.

Endothelial permeability and intercellular boundary

FITC-dextran was used to evaluate cell permeability. The photochemical reaction significantly increased the FITC-dextran flux through the monolayer of HUVEC (Fig. 4a and 4b), indicating a significant development of intercellular gaps.

Fig. 5 shows fluorescence images of β1-integrin distributed over the basal surface of HUVEC observed by TIRF microscopy. Large regions without β1-integrin were observed in HUVEC treated by the photochemical reaction (Fig. 5b), indicating that the reaction lead to large intercellular gaps. The photochemical reaction was also shown to expand the intercellular boundaries of HUVEC.

Capillary structure and morphological change of HUVEC

Fluorescence images of capillary structures in HUVEC were compared before and after the photochemical reaction by staining

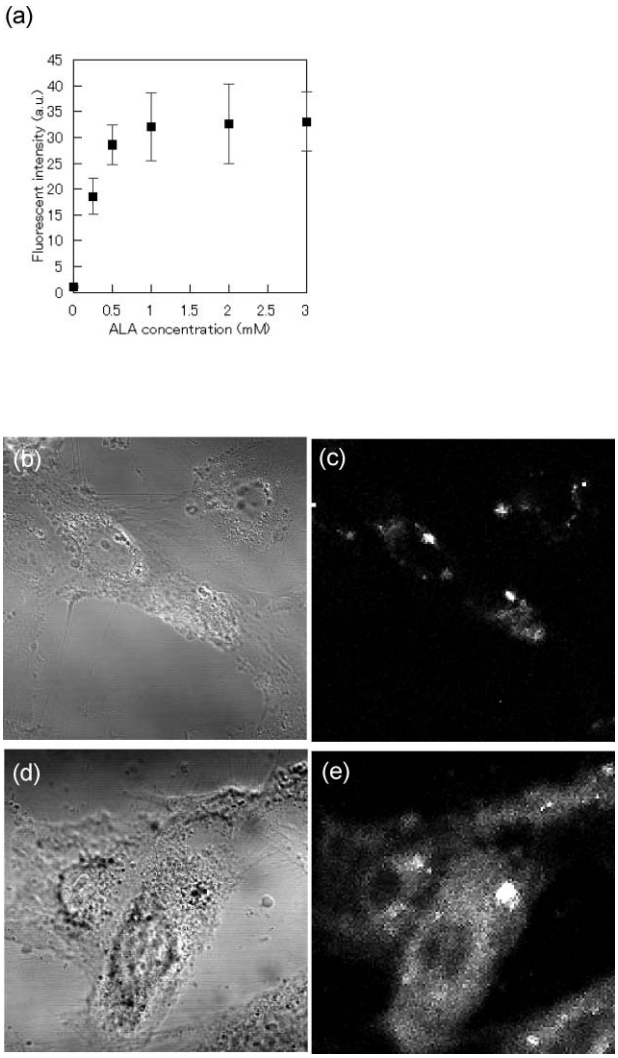

Fig. 2 PpIX in HUVEC. (a) Fluorescence intensity of PpIX as a function of ALA concentration. Optical images of HUVEC (b) before and (d) after 1 mM ALA administration. Fluorescence images of HUVEC (c) before and (e) after 1 mM ALA administration.

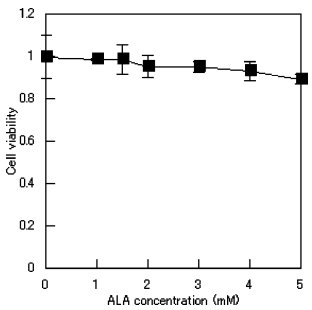

Fig. 3 HUVEC viability with respect to ALA concentration.

with calcein AM (Fig. 6a and 6b). Untreated HUVEC assembled and formed tube-like capillary structures by connecting with each other (Fig. 6a), while treated HUVEC failed to connect together (Fig. 6b). In contrast, treated HUVEC were round in shape. This morphological change in the cells is thought to break down the capillary structure.

View Article Online

Published on 29 July 2009. Downloaded by University of California - Berkeley on 12/01/2015 00:05:04.

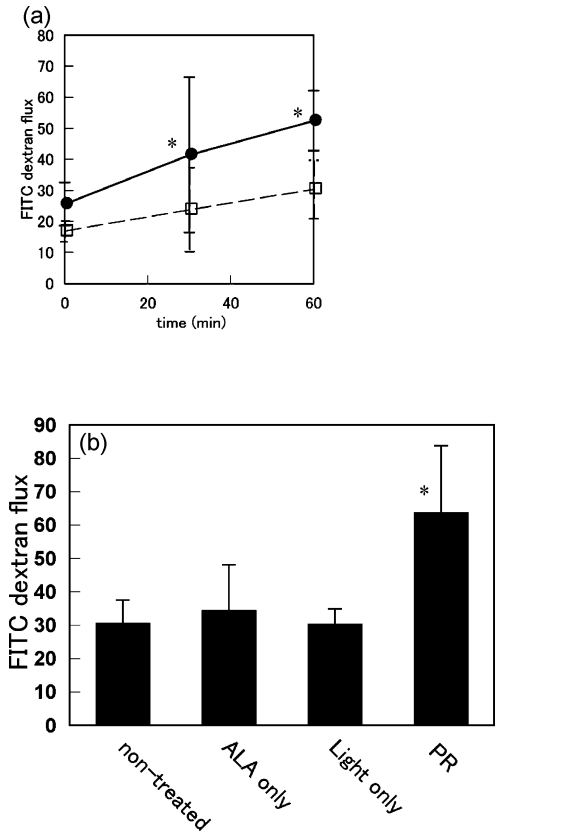

Fig. 4 (a) FITC-dextran flux through the monolayer of HUVEC. FITC-dextran flux across the endothelial monolayer is used as a measure of permeability. Monolayers of HUVEC were treated with (●) or without (□) the photochemical reaction. Values are means ± SD. * $P < 0.05$ *versus* untreated cells. (b) FITC-dextran flux 60 min after the photochemical reaction. Values are means ± SD. * $P < 0.05$ *versus* untreated cells.

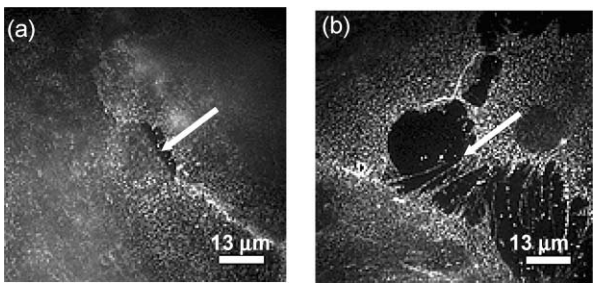

Fig. 5 Fluorescence images of β1-integrin in HUVEC (a) before and (b) after the photochemical reaction.

As shown in Fig. 7, the photochemical reaction caused the monolayers of HUVEC to shrink and thus disconnect from each other. This shrinkage and disconnection increased the subendothelial area (Fig. 7c).

F-actin and VE-cadherin

Fluorescence images of F-actin in HUVEC before and after the photochemical reaction are shown in Fig. 8a and 8b Before the photochemical reaction, F-actin was found mostly in the cortical regions comprising the cortical actin bands, while after the photochemical reaction, these bands rearranged into stress fibers in the center of the cells.

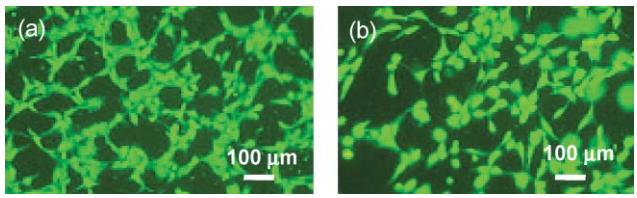

Fig. 6 Fluorescence images of capillary-like structures of HUVEC formed in three-dimensional culture (a) before and (b) after the photochemical reaction.

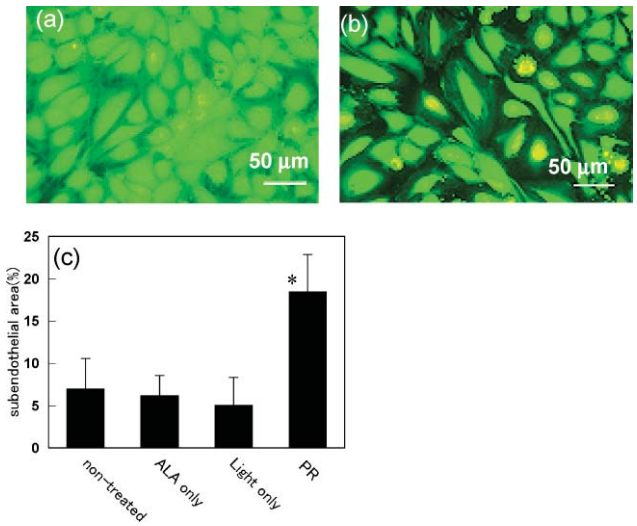

Fig. 7 Fluorescence images of a monolayer of HUVEC (a) before and (b) after the photochemical reaction and (c) the calculated subendothelial areas. Values are means ± SD. * $P < 0.05$ *versus* untreated.

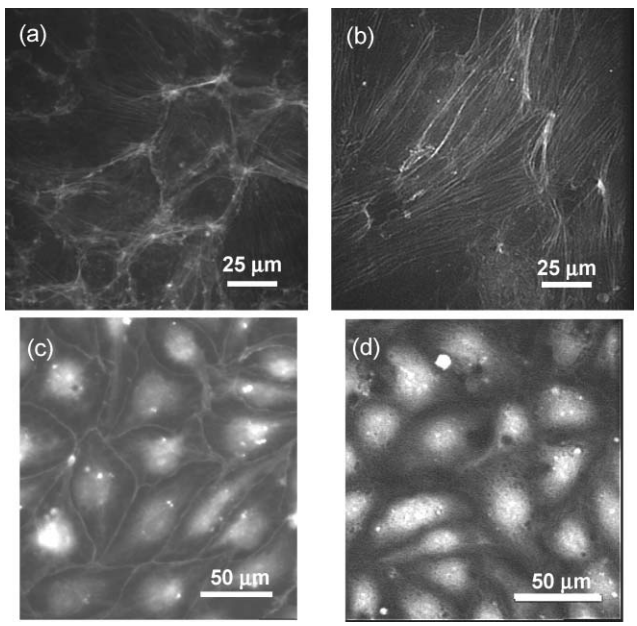

Fig. 8 Fluorescence images of F-actin (a) before and (b) after the photochemical reaction and VE-cadherin (c) before and (d) after the reaction observed by laser scanning confocal microscopy.

Fluorescence images of VE-cadherin in HUVEC before and after the photochemical reaction are shown in Fig. 8c and 8d.

 This journal is © The Royal Society of Chemistry and Owner Societies 2009

View Article Online

Published on 29 July 2009. Downloaded by University of California - Berkeley on 12/01/2015 00:05:04.

VE-cadherin localization at the plasma membrane was not evident after the photochemical reaction.

These results verified that stress fiber formation and VE-cadherin disapperance is correlated with the morphological changes and thus disconnection of the cells.

Rho GTPase

RhoA activation by the photochemical reaction was observed by western blotting (Fig. 9); total RhoA was used as the internal control. Bands of phosphorylated RhoA in cells 0 min, 10 min and 20 min after the photochemical reaction were much stronger than those in untreated cells; the amount of total RhoA was unchanged. These results indicate that the photochemical reaction activated RhoA in HUVEC.

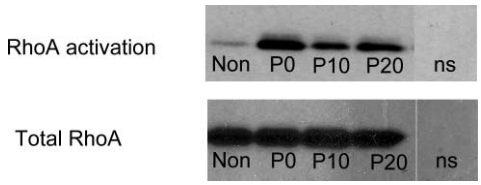

Fig. 9 RhoA activation in response to the photochemical reaction measured by protein activation assays (Non: untreated; P0: 0 min after photochemical reaction; P10: 10 min after photochemical reaction; P20: 20 min after photochemical reaction.)

For the photochemical treatment, cells were incubated with 50 μM forskolin/50 μM rolipram and 500 μM 8-pCPT-2′-O-Me-cAMP both of which are known to prevent RhoA activation by increasing cyclic AMP (cAMP).[10] In both cases, neither endothelial permeability nor subendothelial areas showed an increase (Fig. 10 and 11). Moreover, forskolin and rolipram maintained the cortial actin bands and prevented formation of stress fibers after the photochemical reaction (Fig. 12a and 12b), while 8-pCPT-2′-O-Me-cAMP significantly reduced the effects of the photochemical reaction on HUVEC (Fig. 12c and 12d). These results indicate that RhoA activation is the key factor in increasing endothelial permeability induced by the photochemical reaction.

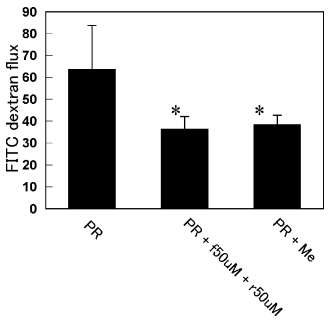

Fig. 10 FITC dextran flux measured 60 min after the photochemical reaction (PR) and PR with 50 μM rolipram/50 μM forskolin (r50 μM + f50 μM) and cAMP analog, 500 μM 8-pCRT-2′-O-Me-cAMP (Me). Values are means ± SD. * $P < 0.05$ *versus* cells after the photochemical reaction.

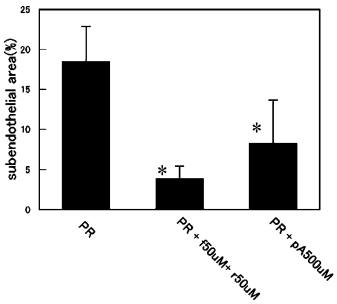

Fig. 11 Subendothelial areas of HUVEC after the photochemical reaction (PR) and PR with 50 μM rolipram/50 μM forskolin (r50 μM + f50 μM) and cAMP analog, 500 μM 8-pCRT-2′-O-Me-cAMP (pA 500 μm) calculated from fluorescence images. Values are means ± SD. * $P < 0.05$ *versus* untreated.

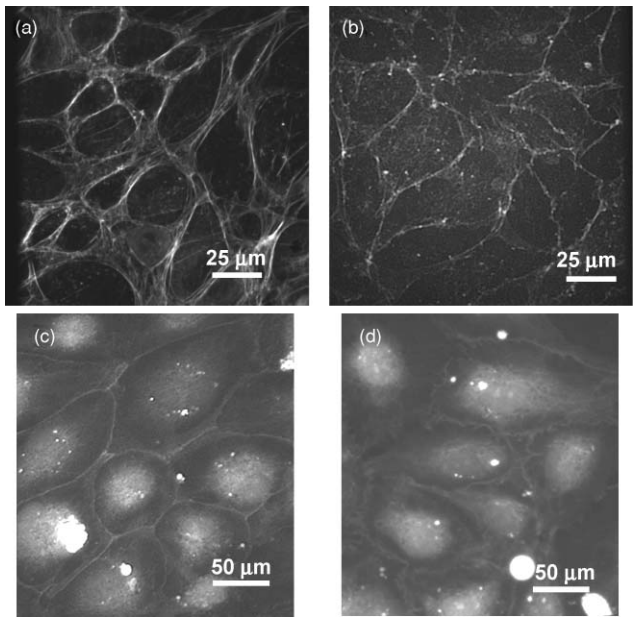

Fig. 12 Fluorescence images of F actin after PR with 50 μM Rolipram/50 μM forskolin (a) and cAMP analog, 500 μM 8-pCRT-2′-O-Me-cAMP (b) and VE-cadherin after PR with 50 μM Rolipram/50 μM forskolin (c) and cAMP analog, 500 μM 8-pCRT-2′-O-Me-cAMP (d) observed by laser scanning confocal microscopy.

Discussion

In this study, we evaluated the increase in endothelial permeability of HUVEC induced by the photochemical reaction using Transwell® supports, bioimaging, and western blotting.

We demonstrated that the amount of PpIX accumulation depended on the ALA concentration in the cell. This effect was obvious for up to 1 mM ALA. Gibson *et al.* reported that the accumulation of PpIX in cells depends on mitochondria density,[11] different cell species appear to affect PpIX accumulation. Our results confirm that PpIX synthesis is localized in the cytoplasm.[12]

To investigate cell viability after the photochemical reaction, we used MTT, as it involves no radioisotopes and is less toxic than WST-1 or trypan blue. The viability of HUVEC showed no significant change at 1 mM ALA, with minimal cell injury by the photoreaction treatment. Spörri *et al.* also reported no difference in the cell number increase after 24 and 48 h between PDT-treated

View Article Online

Published on 29 July 2009. Downloaded by University of California - Berkeley on 12/01/2015 00:05:04.

and untreated cells.[13] Our *in vitro* results that the photochemical reaction increased endothelial permeability supports previous *in vivo* reports of a endothelial barrier breakdown in PDT-treated mice.[7,8] These studies used a transluminal green light and Rose bengal for the photochemical reaction to show that neointimal formation was enhanced after endothelial barrier dysfunction, as our *in vitro* findings suggest using red LEDs.

Upon endothelial barrier breakdown by the photoreaction with ALA, morphological changes of the cells were observed in both the 3D and monolayer cultures. As the breakdown of the capillary structures in the 3D cultures corresponds to a vessel structure *in vivo*, an increase in endothelial permeablity *in vivo* should also lead to morphological changes in the cells.

Increased endothelial permeability *in vivo* can be induced by thrombin,[14] vascular endothelial growth factor,[15] lysophosphatidic acid,[16] high glucose,[17] hypoxia/reoxygenation,[18] and H_2O_2.[19] The administration of thrombin, lysophosphatidic acid (LPA), and hydrogen peroxide (H_2O_2),[20] tumor necrosis factor (TNF)-α,[21] and monocyte chemotactic protein (MCP)-1[22] *in vitro* also induces rearrangement of the cytoskelton F-actin and disappearance of VE-cadherin, which are events that upregulate endothelial permeability. Analysis of F-actin and VE-cadherin using fluorescence imaging revealed that F-actin in cortical actin bands on the periphery of cells disappeared and were rearranged into stress fibers. Loss of cortical actin bands and formation of stress fibers have been reported to be caused by shear stress[23] and by ROS produced *via* hypoxia/reoxygenation.[24] Thus, in our *in vitro* experiments, the cortical actin band loss associated with the formation of stress fibers appears to be a result of ROS produced by the photoreaction.

Similar to the association of actin filament formation with drastic cell morphology changes caused by the photoreaction, another cytoskeleton microtubule has also been reported to play a key role, as they regulate the phosphorylation of the myosin light chains that form stress fibers.[25–27]

Among the endothelial cell–cell junctions, tight junctions, adherence junctions, or gap junctions, adherence junctions with VE-cadherin have been reported to be the most critical for increasing endothelial permeability.[28] We found that gaps between cells are expand by the photoreaction following the disappearance of VE-cadherin on the periphery of cells. VE-cadherin is anchored to the actin filament by several intermediate catenins (α β and γ),[29,30,31] indicating that correlation between the disappearance of VE-cadherin and the loss of the cortical actin band.

We observed β1-integrin on the plasma membrane by TIRF fluorescence microscopy. β1-Integrin which adheres the cells to the basal surface disappeared in large areas after the photoreaction treatment, indicating a drastic reduction in the surface areas of cell–cell adhesion.[32]

The intercellular signaling pathway in charge of the formation of stress fibers and regulation of adherence junctions depends on cell species and the applied stimulations.[14,18,33,34,35] Two Rho GTPases RhoA and Rap1 have been reported to be important in the signaling pathway involved in increasing endothelial permeability.[36] RhoA activation has been reported to lead to increased endothelial permeability by forming stress fibers and tubulin depolymerization when cells are exposed to thrombin.[37] We used western blotting to evaluate RhoA activity in endothelial cells stimulated by the photoreaction and found that RhoA activation played a key role in the induced increase in endothelial permeability.

Increases in endogenous cAMP activates Epacs and, subsequently, Rap1, a downregulator of RhoA activation.[10] PKA is also activated by cAMP, and we demonstrated that cAMP prevented the formation of stress fibers and the rearrangement of VE-cadherin. The cAMP analog 8-pCRT-2′-O-Me-cAMP, which selectively activates Epacs and does not affect PKA activation, was also found to prevent the photoreaction-induced increase in endothelial permeability. Three Rho GTPases—RhoA, Rac1, and Rap1—have been reported to be cross-linked and not independent.[38] Whereas ROS generated by the photochemical reaction cause cell shrinkage and VE-cadherin rearrangement and thus increases endotherial permeability, ROS generated by reoxygeneration have been reported to activate Rac1, inhibiting RhoA activation and thus not increasing endothelial permeability.[18] Activation of RhoGTPase may depend on the amount of ROS, and the method of regulation may differ depending on the species. Thus, designing a more effective PDT with fewer side effects requires medicine that prevent activation of RhoA immediately after therapy.

Conclusions

In vitro experiments using HUVEC revealed the mechanisms by which endothelial permeability is increased by the photoreaction treatment with ALA. The accumulation of PpIX in the cytoplasm is the greatest at 1 mM ALA, a dose level that does not significantly decrease cell viability. The photochemical reaction with 1 mM ALA using a 646 nm light at 10 mW cm^{-2} significantly increased the endothelial permeability of both monolayer and 3D cultures of HUVEC, the latter having capillary shapes. This increase is accompanied by morphological changes in the cells. The cortical actin bands on the periphery of cells rearrange into stress fibers in the center of the cells and VE-cadherin disappears, which causes the morphological changes in the cells. RhoA activation plays a key role in the photochemical reaction, as confirmed by the *in vitro* results using cAMP to inhibit RhoA activation.

In summary, the photochemical reaction induces the increase in endothelial permeability, by activating RhoA, causing the breaking down of the cortical actin band to form stress fibers, and then rearranging VE-cadherin, all of which leading to changes in cell morphology.

References

1 R. L. Lipton, E. J. Baldes and A. M. Olsen, Hematoporphyrin derivative: a new aid for endoscopic detection of malignant disease, *J. Thorac. Cardiovasc. Surg.*, 1961, **42**, 623–629.
2 Z. Malik and H. Lugaci, Destruction of erythroleukaemic cells by photoactivation of endogenous porphyrins, *Br. J. Cancer*, 1987, **56**, 589–595.
3 J. C. Kennedy, R. H. Pottier and D. C. Pross, Photodynamic therapy with endogenous protoporphyrin IX: basic principles and present clinical experience, *J. Photochem. Photobiol., B*, 1990, **6**, 143–148.
4 J. Webber, Y. Luo, R. Crilly, D. Fromm and D. Kessel, An apoptotic response to photodynamic therapy with endogenous protoporphyrin in vivo, *J. Photochem. Photobiol., B*, 1996, **35**, 209–211.
5 V. H. Fingar, Vascular effects of photodyanamic therapy, *J. Clin. Laser Med. Surg.*, 1996, **14**(5), 323–328.
6 S. Mennel, S. Peter, C. H. Meyer and G. Thumann, Effect of photodynamic therapy on the function of the outer blood-retinal

 This journal is © The Royal Society of Chemistry and Owner Societies 2009

View Article Online

Published on 29 July 2009. Downloaded by University of California - Berkeley on 12/01/2015 00:05:04.

barrier in an in vitro model, *Graefe's Arch. Clin. Exp. Ophthalmol.*, 2006, **244**, 1015–21.
7 S. Kikuchi, K. Umemura, K. Kondo, A. R. Saniabadi and M. Nakashima, Photochemically induced endothelial injury in the mouse as a screening model for inhibitors of vascular intimal thickening, *Arterioscler., Thromb., Vasc. Biol.*, 1998, **18**, 1069–78.
8 M. Shimazawa, S. Watanabe, K. Kondo, H. Hara, M. Nakashima and K. Umemura, Neutrophil accumulation promotes intimal hyperplasia after photochemically induced arterial injury in mice., *Eur. J. Pharmacol.*, 2005, **520**, 156–63.
9 B. Grandchamp, J. C. Deybach, M. Grelier, H. de Verneuil and Y. Nordmann, Studies of porphyrin synthesis in fibroblasts of patients with congenital erythropoietic porphyria and one patient with homozygous coproporphyria., *Biochim. Biophys. Acta, Gen. Subj.*, 1980, **629**, 577–86.
10 X. Cullere, S. K. Shaw, L. Andersson, J. Hirahashi, F. W. Luscinskas and T. N. Mayadas, Regulation of vascular endothelial barrier function by Epac, a cAMP-activated exchange factor for Rap GTPase., *Blood*, 2005, **105**, 1950–5.
11 S. L. Gibson, M. L. Nguyen, J. J. Havens, A. Barbarin and R. Hilf, Relationship of delta-aminolevulinic acid-induced protoporphyrin IX levels to mitochondrial content in neoplastic cells in vitro., *Biochem. Biophys. Res. Commun.*, 1999, **265**, 315–321.
12 Z. Ji, G. Yang, V. Vasovic, B. Cunderlikova, Z. Suo, J. M. Nesland and Q. Peng, Subcellular localization pattern of protoporphyrin IX is an important determinant for its photodynamic efficiency of human carcinoma and normal cell lines., *J. Photochem. Photobiol., B*, 2006, **84**, 213–20.
13 S. Spörri, V. Chopra, N. Egger, H. K. Hawkins, M. Motamedi, E. Dreher and H. Schneider, Effects of 5-aminolaevulinic acid on human ovarian cancer cells and human vascular endothelial cells in vitro., *J. Photochem. Photobiol., B*, 2001, **64**, 8–20.
14 S. Fukuhara, A. Sakurai, H. Sano, A. Yamagishi, S. Somekawa, N. Takakura, Y. Saito, K. Kangawa and N. Mochizuki, Cyclic AMP potentiates vascular endothelial cadherin-mediated cell-cell contact to enhance endothelial barrier function through an Epac-Rap1 signaling pathway., *Mol. Cell. Biol.*, 2005, **25**, 136–46.
15 A. M. Geerts, A. S. De Vriese, E. Vanheule, H. Van Vlierberghe, S. Mortier, K. J. Cheung, P. Demetter, N. Lameire, M. De Vos and I. Colle, Increased angiogenesis and permeability in the mesenteric microvasculature of rats with cirrhosis and portal hypertension: an in vivo study., *Liver Int.*, 2006, **26**, 889–98.
16 G. P. van Nieuw Amerongen, M. A. Vermeer and V. W. van Hinsbergh, Role of RhoA and Rho kinase in lysophosphatidic acid-induced endothelial barrier dysfunction., *Arterioscler., Thromb., Vasc. Biol.*, 2000, **20**, E127–33.
17 F. Pricci, G. Leto, L. Amadio, C. Iacobini, S. Cordone, S. Catalano, A. Zicari, M. Sorcini, U. Di Mario and G. Pugliese, Oxidative stress in diabetes-induced endothelial dysfunction involvement of nitric oxide and protein kinase C., *Free Radical Biol. Med.*, 2003, **35**, 683–94.
18 B. Wojciak-Stothard, L. Y. Tsang and S. G. Haworth, Rac and Rho play opposing roles in the regulation of hypoxia/reoxygenation-induced permeability changes in pulmonary artery endothelial cells, *Am. J. Physiol.: Lung Cell. Mol. Physiol.*, 2005, **288**, L749–60.
19 K. S. Lee, S. R. Kim, S. J. Park, H. S. Park, K. H. Min, M. H. Lee, S. M. Jin, G. Y. Jin, W. H. Yoo and Y. C. Lee, Hydrogen peroxide induces vascular permeability *via* regulation of vascular endothelial growth factor., *Am. J. Respir. Cell Mol. Biol.*, 2006, **35**, 190–197.
20 M. P. Gupta, H. O. Steinberg and C. M. Hart, H2O2 causes endothelial barrier dysfunction without disrupting the arginine-nitric oxide pathway., *Am. J. Physiol.: Lung Cell. Mol. Physiol.*, 1998, **274**, L508–16.
21 B. Wójciak-Stothard, A. Entwistle, R. Garg and A. J. Ridley, Regulation of TNF-alpha-induced reorganization of the actin cytoskeleton and cell-cell junctions by Rho, Rac, and Cdc42 in human endothelial cells., *J. Cell. Physiol.*, 1998, **176**, 150–65.
22 Svetlana M. Stamatovic, Oliver B. Dimitrijevic, Richard F. Keep and Anuska V. Andjelkovic, Protein Kinase Cα-RhoA Cross-talk in CCL2-induced Alterations in Brain Endothelial Permeability, *J. Biol. Chem.*, 2006, **281**, 8379–8388.
23 M. Yoshigi, L. M. Hoffman, C. C. Jensen, H. J. Yost and M. C. Beckerle, Mechanical force mobilizes zyxin from focal adhesions to actin filaments and regulates cytoskeletal reinforcement., *J. Cell Biol.*, 2005, **171**, 209–15.
24 C. A. Partridge, Hypoxia and reoxygenation stimulate biphasic changes in endothelial monolayer permeability., *Am. J. Physiol.: Lung Cell. Mol. Physiol.*, 1995, **269**, L52–L58.
25 Anna A. Birukova, Feng Liu, Joe G. N. Garcia and Alexander D. Verin, Protein kinase A attenuates endothelial cell barrier dysfunction induced by microtubule dissaembly, *Am. J. Physiol.: Lung Cell. Mol. Physiol.*, 2004, **287**, L86–L93.
26 I. Petrache, A. Birukova, S. I. Ramirez, J. G. Garcia and A. D. Verin, The role of the microtubules in tumor necrosis factor-alpha-induced endothelial cell permeability., *Am. J. Respir. Cell Mol. Biol.*, 2003, **28**, 574–81.
27 M. N. Bijman, G. P. van Nieuw Amerongen, N. Laurens, V. W. van Hinsbergh and E. Boven, Microtubule-targeting agents inhibit angiogenesis at subtoxic concentrations, a process associated with inhibition of Rac1 and Cdc42 activity and changes in the endothelial cytoskeleton., *Mol. Cancer Ther.*, 2006, **5**, 2348–57.
28 N. Matsuyoshi, K. Toda, Y. Horiguchi, T. Tanaka, S. Nakagawa, M. Takeichi and S. Imamura, In vivo evidence of the critical role of cadherin-5 in murine vascular integrity, *Proc. Assoc. Am. Physicians*, 1997, **109**, 362–371.
29 B. M. Gumbiner, Cell adhesion : the molecular basis of tissue architecture and morphogenesis., *Cell*, 1996, **84**, 345–357.
30 L. Hinck, I. S. Natheke, J. Papkoff and W. J. Nelson, Dynamics of cadherin/catenin complex formation: novel protein interactions and pathways of complex assembly, *J. Cell Biol.*, 1994, **125**, 1327–1340.
31 J. E. Nieset, A. R. Redfield, F. Jin, K. A. Knudsen, K. R. Johnson and M. J. Wheelock, Characterization of the interactions of α-actinin and β-catenin/plakoglobin., *J. Cell Sci.*, 1997, **110**, 1013–1022.
32 K. Kawakami, H. Tatsumi and M. Sokabe, Dynamics of integrin clustering at focal contacts of endothelial cells studied by multimode imaging microscopy., *J. Cell Sci.*, 2001, **114**, 3125–35.
33 S. van Wetering, J. D. van Buul, S. Quik, F. P. Mul, E. C. Anthony, J. P. ten Klooster, J. G. Collard and P. L. Hordijk, Reactive oxygen species mediate Rac-induced loss of cell-cell adhesion in primary human endothelial cells., *J. Cell Sci.*, 2002, **115**, 1837–46.
34 B. Wójciak-Stothard, S. Potempa, T. Eichholtz and A. J. Ridley, Rho and Rac but not Cdc42 regulate endothelial cell permeability, *J. Cell Sci*, 2001, **114**, 1343–55.
35 W. T. Arthur, L. A. Quilliam and J. A. Cooper, Rap1 promotes cell spreading by localizing Rac guanine nucleotide exchange factors, *J. Cell Biol.*, 2004, **167**, 111–22.
36 Dolly Mehta and Asrar B. Malik, Signaling Mechanisms Regulating Endothlial Permeability, *Physiol. Rev.*, 2006, **86**(1), 279–367.
37 A. A. Birukova, K. G. Birukov, K. Smurova, D. Adyshev, K. Kaibuchi, I. Alieva, J. G. Garcia and A. D. Verin, Novel role of microtubules in thrombin-induced endothelial barrier dysfunction, *FASEB J.*, 2004, **18**, 1879–90.
38 E. E. Evers, G. C. Zondag, A. Malliri, L. S. Price, J. P. ten Klooster, R. A. van der Kammen and J. G. Collard, Rho family proteins in cell adhesion and cell migration., *Eur. J. Cancer*, 2000, **36**, 1269–74.